Semicond. Sci. Technol. **23** (2008) 035003 (6pp) doi:10.1088/0268-1242/23/3/035003

The distribution of the barrier height in Al–TiW–Pd_2Si/n-Si Schottky diodes from *I–V–T* measurements

İlbilge Dökme[1], Şemsettin Altındal[2] and İzzet M Afandiyeva[3]

[1] Science Education Department, Faculty of Education, Ahi Evran University, Kırşehir, Turkey
[2] Physics Department, Faculty of Arts and Sciences, Gazi University, 06500, Teknikokullar, Ankara, Turkey
[3] Institute of Physics Problems, Bakü State University, AZ 1148, Baku, Azerbaijan

Received 19 August 2007, in final form 16 December 2007
Published 31 January 2008
Online at stacks.iop.org/SST/23/035003

Abstract

The forward and reverse bias current–voltage (*I–V*) characteristics of Al–TiW–Pd_2Si/n-Si Schottky barrier diodes (SBDs) were measured in the temperature range of 300–400 K. The estimated zero-bias barrier height Φ_{B0} and the ideality factor n assuming thermionic emission (TE) theory show a strong temperature dependence. While n decreases, Φ_{B0} increases with increasing temperature. The Richardson plot is found to be linear in the temperature range measured, but the activation energy value of 0.378 eV and the Richardson constant (A^*) value of 15.51 A cm^{-2} K^{-2} obtained in this plot are much lower than the known values. Such behavior is attributed to Schottky barrier inhomogeneities by assuming a Gaussian distribution of barrier heights (BHs) due to BH inhomogeneities that prevail at the interface. Also, the Φ_{B0} versus $q/2kT$ plot was drawn to obtain evidence of a Gaussian distribution of the BHs, and $\Phi_{B0} = 0.535$ eV and $\sigma_0 = 0.069$ V for the mean BH and zero-bias standard deviation, respectively, have been obtained from this plot. Thus, the modified $\ln(I_0/T^2) - q^2\sigma_0^2/2k^2T^2$ versus q/kT plot gives Φ_{B0} and A^* as 0.510 eV and 121.96 A cm^{-2} K^{-2}, respectively. This value of the Richardson constant 121.96 A cm^{-2} K^{-2} is very close to the theoretical value of 120 A K^{-2} cm^{-2} for n-type Si. Hence, it has been concluded that the temperature dependence of the forward *I–V* characteristics of the Al–TiW–Pd_2Si/n-Si Schottky barrier diodes can be successfully explained on the basis of a thermionic emission mechanism with a Gaussian distribution of the BHs.

1. Introduction

Palladium silicide films are commonly used in the fabrication of Schottky barriers and ohmic contacts in silicon devices. Because of the importance of metal silicides in integrated circuit technology, Pd_2Si films on Si have received a lot of attention in the past. The first studies on Pd_2Si films were made by Kircher [1], who investigated the metallurgical properties and electrical characteristics of Pd_2Si contacts on n-Si. Wittmer *et al* [2] and Shepela [3] performed the measurement of the resistivity of a Pd_2Si film grown on a Si substrate. Extensive studies were carried out on the growth kinetics, composition and electrical properties of the Pd_2Si film on Si [4–15]. After new industrial applications including an infrared detector and sensor in thermal imaging devices had been carried out, the studies on them were pursued with vigor [16–19]. Chand and Kumar [20–23] have analyzed the current–voltage (*I–V*) characteristics of Pd_2Si-based Schottky diodes on n-Si and p-Si. They interpreted the abnormal *I–V* characteristics on the basis of thermionic emission–diffusion theory (TED) and the assumption of a Gaussian distribution of barrier heights. The reaction between the top metal conductor and the silicide can be responsible for the abnormal characteristics of palladium silicide-based Schottky diodes especially at high temperature. An attempt has, therefore, been made in this study to prevent the disadvantage of Al diffusion into Si. For case studies, Al–TiW–Pd_2Si/n-Si diodes were fabricated and measured over the temperature range of 300–400 K.

In our previous study [24], we studied the frequency dependence of the forward and reverse bias *C–V* and G/w–*V* and *I–V* characteristics of Al–TiW–Pd_2Si/n-Si structures at

room temperature. Only at room temperature the analysis of *I–V* characteristics cannot give detailed information about the current conduction mechanism and structural parameters of devices. Therefore, in this study, the *I–V* characteristics of Al–TiW–Pd_2Si/n-Si structures have been investigated in the temperature range of 300–400 K. The first aim of this study is to investigate whether the top conductor, aluminum, is responsible for the abnormal behavior of the *I–V* characteristic. Therefore, a layer of Ti–W (10% Ti, 90% W) was sputter coated between the palladium silicide and metal interconnects. The W here acts as a barrier and hinders the diffusion of Si into Al while Ti allows the Ti–W layer to adhere well to the oxide. However, the experimental results show that the barrier height and ideality factor determined from forward bias *I–V* characteristics were found to be a strong function of temperature. The ideality factor n was found to decrease while the SBH increases with increasing temperature. The temperature dependence of Schottky barrier characteristics of the diodes was interpreted on the basis of the existence of the Gaussian distribution of the BHs around a mean value due to BH inhomogeneities prevailing at the silicide–semiconductor interface.

2. Experimental procedure

The Al–TiW–Pd_2Si/n-Si structures were fabricated on a 2 inch diameter n-type (P doped) single crystal silicon wafer with (1 1 1) surface orientation, 0.7 Ω cm resistivity and 3.5 μm thickness. The pattern of these structures was formed by a photolithographic technique, and annealed at 773 K for 1 min in flowing dry nitrogen (N_2) ambient in a rapid thermal annealing furnace. Thus produced chip contains 14 Al–TiW–Pd_2Si/n-Si structures with the rectifier contact areas between 1×10^{-6} cm^2 and 14×10^{-6} cm^2. Only the results for the diode with the area of 8×10^{-6} cm^2 are presented in this paper.

For the fabrication process, the Si wafer was first cleaned in a mix of peroxide–ammoniac solution for 10 min and subsequently quenched in de-ionized water of resistivity 18 MΩ cm for a prolonged time. After the cleaning process, high-purity (99.999%) Al with a thickness of about 2000 Å was thermally evaporated onto the whole back side of the Si wafer at a pressure of about 10^{-6} Torr in a high vacuum system. The ohmic contacts were formed by annealing them for a few minutes at 723 K. To fabricate the Pd_2Si layer, palladium was deposited on the Si wafer by using the thermal evaporation method at 523 K. At this temperature, the Pd deposited on the contact regions reacts to form Pd_2Si. The unconverted Pd was etched away with an aqueous solution of KI + I_2, an etchant which does not attack Pd_2Si, and subsequently annealed at 573 K for 15 min. The thickness of Pd_2Si was determined to be about 0.6 μm by the use of the spectroscopic ellipsometry system (Jobin Yvon-Horiba). To form the metal electrodes (rectifier and ohmic contacts), traditionally Al dots could have been formed on the Pd_2Si–n-Si structure. But Al has high diffusion ability and it can lead to degradation of the contacts' quality. Therefore, in this work, to prevent the disadvantage of Al diffusion into Si, the TiW alloy played the role of a diffusion barrier between Pd_2Si and Al, and was deposited on the Pd_2Si–n-Si layer. For this process, the sandwiched structure Al–$Ti_{10}W_{90}$ was deposited by the magnetron sputtering method at a substrate temperature of 693 K in the vacuum system 'Oratoria-5' and then annealed at a temperature of 773 K in nitrogen atmosphere (N_2) for 20 min.

Prior to the deposition, vacuum and target conditions were performed. Taking into account the dispersion factors of Ti and W, a compound target (Ti 10%, W 90%) was made. The deposition chamber was pumped down to the ultimate vacuum and repeatedly charged with argon in order to minimize the residual gas components. The alloy compound target film was bombarded by Ar^+ ions with high energy at room temperature. The base pressure during the ion bombardments was about 10^{-6} Torr. Al was also deposited onto the TiW–Pd_2Si/n-Si structure by the same method until the thickness of the Al film on the $Ti_{10}W_{90}$–Pd_2Si–n-Si layer was about 1 μm.

The temperature dependence of current–voltage–temperature (*I–V–T*) measurements was performed by the use of a Keithley 220 programmable constant current source together with a Keithley 614 electrometer in a Janes vpf-475 cryostat with the Lake Shore model 321 auto-tuning temperature controllers in a vacuum of 5×10^{-4} Torr. All measurements were carried out with the help of a microcomputer through an IEEE-488 ac/dc converter card.

3. Results and discussions

3.1. The analysis of the barrier height and Richardson constant from I–V–T characteristics

Figure 1 shows the semi-logarithmic *I–V* characteristics of the Al–TiW–Pd_2Si/n-Si Schottky barrier diodes, measured at different temperatures over the range of 300–400 K. It can be seen that the current rises slowly with the applied reverse bias and does not show any effect of saturation. This 'soft' or slight non-saturation behavior observed as a function of bias in the experimental reverse bias branch in figure 1 may be explained in terms of spatial inhomogeneity of SBH [25–27]. For the inhomogeneous Schottky contacts, the reverse current may be dominated by the current which flows through the low-SBH patches, which is controlled by the potential at the saddle point. Increasing reverse bias drops the potential at the saddle point; hence the reverse current increases with increasing reverse bias and does not saturate. The current through a SBD at a forward bias ($V \geqslant 3kT/q$), according to TE theory, is given by [28]

$$I = I_0 \exp\left(\frac{qV}{nkT}\right)\left[1 - \exp\left(-\frac{qV}{kT}\right)\right] \tag{1}$$

where I_0 is the reverse saturation current derived from the straight-line intercept of ln I at zero bias and is defined by

$$I_0 = A\ A^*\ T^2\ \exp\left(-\frac{q\Phi_{B0}}{kT}\right) \tag{2}$$

where q is the electronic charge, A^* is the effective Richardson constant and is equal to 264 A cm^{-2} K^{-2} for n-type Si, A is the effective diode area, k is the Boltzmann constant, T is the absolute temperature in K, Φ_{B0} is the zero-bias barrier height and n is the ideality factor. The ideality factor is calculated

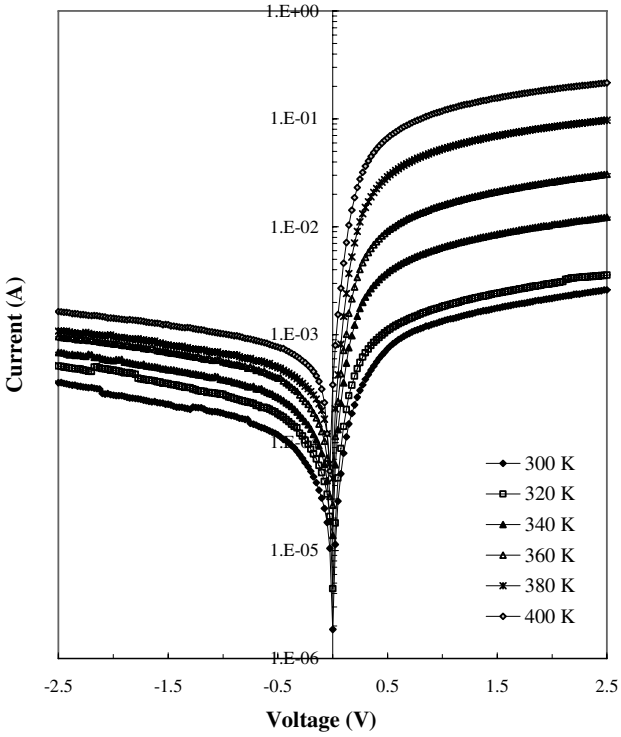

Figure 1. The experimental forward bias *I–V* characteristics of the Al–TiW–Pd_2Si/n-Si Schottky barrier diodes at various temperatures.

from the slope of the linear region of the forward bias ln(*I*)–*V* plot and can be written from equation (1) as

$$n = \frac{q}{kT}\left(\frac{\mathrm{d}V}{\mathrm{d}(\ln I)}\right). \tag{3}$$

Also, the voltage-dependent ideality factor can be written from equation (1) as

$$n(V) = \frac{qV}{kT\ln(I/I_0)}. \tag{4}$$

The zero-bias barrier height Φ_{B0} ($=\Phi_B(I\text{–}V)$) is determined from the extrapolated I_0 and is given by

$$\Phi_{B0} = \frac{kT}{q}\ln\left[\frac{AA^*T^2}{I_0}\right]. \tag{5}$$

The experimental values of n and Φ_{B0} were determined from equations (3) and (5), respectively, and shown in table 1 for each temperature. As shown in table 1, Φ_{B0} and n for the Al–TiW–Pd_2Si/n-Si Schottky barrier diode ranged from 0.462 eV and 1.28 (at 400 K) to 0.436 eV and 2.03 (at 300 K), respectively. That is to say the values of Φ_{B0} and n are strong functions of temperature.

The values of the ideality factor n decrease with increasing temperature and are greater than unity at each temperature. Such behavior of the ideality factor has been attributed to the particular distribution of interface states and the insulator layer between metal and semiconductor [28–38].

The values of Φ_{B0} increase with increasing temperature. Similar results have been reported in the literature [8, 13, 21]. Such a temperature dependence is in obvious disagreement with the reported negative temperature coefficient of the

Table 1. Temperature-dependent values of various diode parameters determined from the *I–V* characteristics of Al–TiW–Pd_2Si/n-Si Schottky barrier diodes in the temperature range of 300–400 K.

T (K)	I_0 (A)	n	Φ_{B0} (eV)	Φ_{bf} (eV)
300	6.98×10^{-6}	2.03	0.436	0.658
320	1.12×10^{-5}	1.73	0.455	0.616
340	3.37×10^{-5}	1.67	0.455	0.592
360	6.74×10^{-5}	1.50	0.464	0.564
380	1.83×10^{-4}	1.40	0.460	0.532
400	3.90×10^{-4}	1.28	0.462	0.508

Schottky barrier height. Since the current transport across the metal semiconductor interface is a temperature-activated process, electrons are able to surmount the lower barriers. Therefore, the current flow through the lower SBH and a larger ideality factor will dominate current transport. In other words more electrons have sufficient energy to overcome the higher barrier when the BH builds up with increasing temperature and bias voltage. This result is attributed to inhomogeneous interfaces and barrier heights because there is a linear relationship between the barrier height and ideality factor (figure 3). Also Schmitsdorf *et al* [34] used Tung's [27] theoretical approach and they found a linear correlation between the experimental zero-bias SBHs and ideality factors. However, the barrier height obtained under a flat-band condition is considered to be a real fundamental quantity. Unlike the case of the zero-bias barrier height, the electrical field in a semiconductor is zero under the flat-band condition. This eliminates the effect of the image force lowering that would affect the *I–V* characteristics, and removes the influence of lateral inhomogeneity [38]. The flat-band barrier height Φ_{bf} can be calculated from the experimental ideality factor and zero-bias BH Φ_{B0} according to [20–23]

$$\Phi_{bf} = n\phi_{B0} - (n-1)\frac{kT}{q}\ln\left(\frac{N_C}{N_D}\right) \tag{6}$$

where N_C is the effective density of states in the conductivity band and N_D is the carrier doping density of n-type Si with 5.86×10^{15} cm^{-3}. A plot of Φ_{bf} as a function of temperature is shown in figure 2. As shown in figure 2, the temperature dependence of the flat-band BH can be expressed as

$$\Phi_{bf}(T) = \Phi_{bf}(T=0) + \alpha T \tag{7}$$

where Φ_{bf} is the flat-band BH extrapolated to $T = 0$ K and α is its temperature coefficient. In figure 2, the fitting of $\Phi_{bf}(T)$ data in equation (7) yields $\Phi_{bf}(T=0) = 1.5$ eV and $\alpha = -2 \times 10^{-3}$ eV K^{-1}.

Figure 3 shows a plot of the experimental BH versus the ideality factor for various temperatures. The straight line in figure 3 is the least-squares fit to the experimental data. As can be seen from figure 3, there is a linear relationship between the experimental effective BHs and the ideality factors of the Schottky contact that was explained by lateral inhomogeneities of the BHs in the Schottky diodes [34]. The extrapolation of the experimental BHs versus ideality factors plot to $n = 1$ has given a homogeneous BH of approximately 0.483 eV. Thus, it can be said that the significant decrease of the zero-bias BH

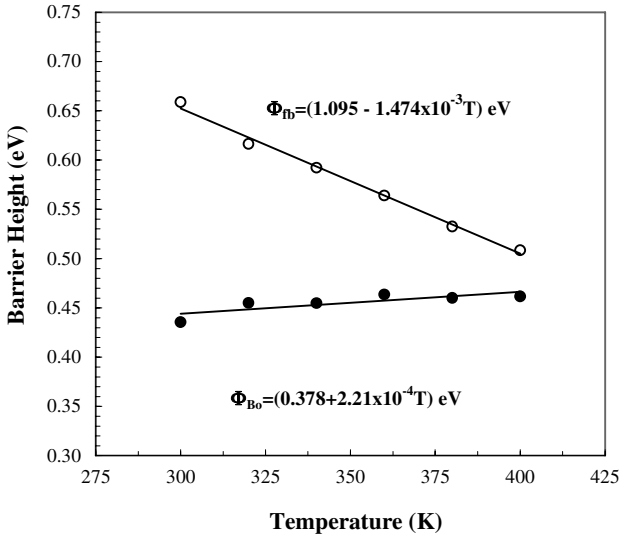

Figure 2. Temperature dependence of the zero-bias barrier height and the flat-band barrier height for Al–TiW–Pd_2Si/n-Si Schottky barrier diodes.

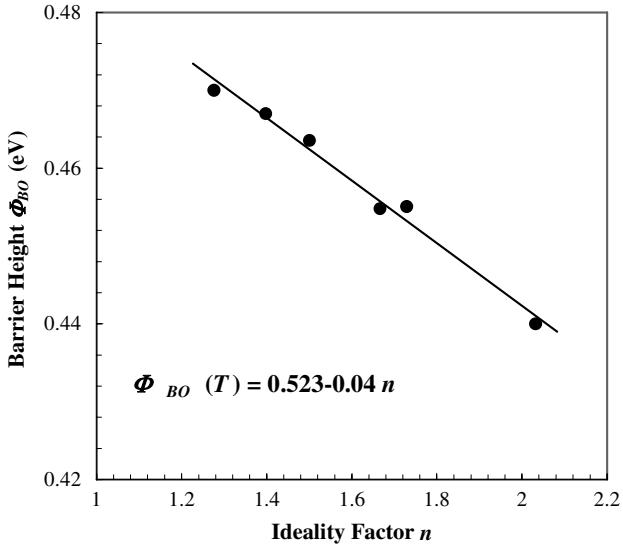

Figure 3. Linear variation of the apparent barrier height versus ideality factors at various temperatures.

and increase of the ideality factor especially at low temperature are possibly caused by the BH inhomogeneities.

To evaluate the BH in another way, we use the Richardson plot of the reverse saturation current I_0. By taking the natural logarithm of equation (2), one can obtain

$$\ln\left(\frac{I_0}{T^2}\right) = \ln(AA^*) - \frac{q\Phi_{B0}}{kT}. \tag{8}$$

The conventional energy variation of the $\ln(I_0/T^2)$ versus $1000/T$ plot is found to be linear in the temperature range measured as shown in figure 5. When the experimental data are fit asymptotically with a straight line it yields an activation energy of 0.369 eV. Likewise, a Richardson constant (A^*) value

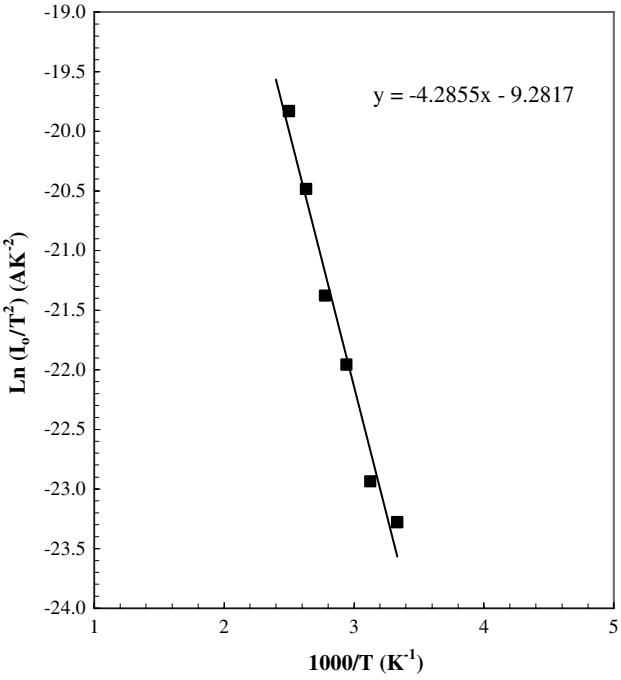

Figure 4. Richardson plots of $\ln(I_0/T^2)$ versus $1000/T$ for the Al–TiW–Pd_2Si/n-Si Schottky barrier diode.

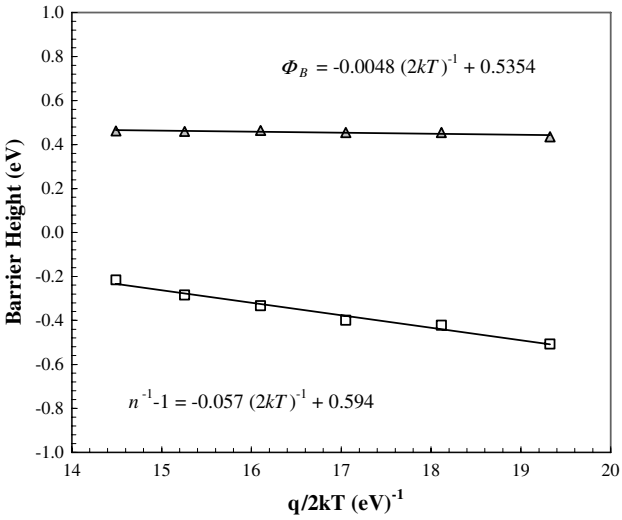

Figure 5. Zero-bias apparent barrier height and ideality factor versus $1/T$ curves of the Al–TiW–Pd_2Si/n-Si Schottky diode according to the Gaussian distribution of the barrier height.

of 15.46 A cm^{-2} K^{-2} for the Al–TiW–Pd_2Si/n-Si Schottky barrier diode was determined from the intercept at the ordinate of the experimental $\ln(I_0/T^2)$ versus $1000/T$ plot in figure 4. This value is about eight times lower than the known value of 120 A cm^{-2} K^{-2} for n-Si [30]. This deviation in A^* may be due to the spatial inhomogeneous barrier heights and potential fluctuation at the interface that consist of low and high barrier areas [35–38]. Furthermore, the value of the Richardson constant obtained from the *I–V* characteristics as a function

of temperature may be affected by the lateral inhomogeneity of the barrier.

3.2. The analysis of the inhomogeneous barrier and modified Richardson plot

To explain the commonly observed abnormal deviation from classical thermionic emission theory, some authors [20–22, 27] have considered a system of discrete region of low barrier imbedded in a higher background uniform barrier. This abnormal behavior can be explained by assuming a Gaussian distribution of the barrier height with a mean value $\bar{\Phi}_{B0}$ and standard deviation σ_s, which can be given as [20–22, 29, 32, 37, 39–42]

$$P(\Phi_B) = \frac{1}{\sigma_s\sqrt{2\pi}} \exp\left[-\frac{(\Phi_B - \bar{\Phi}_B)^2}{2\sigma_s^2}\right] \tag{9}$$

where $1/\sigma_s\sqrt{2\pi}$ is the normalization constant of the Gaussian barrier height distribution. The total $I(V)$ across a Schottky diode containing barrier inhomogeneities can be expressed as

$$I(V) = \int_{-\infty}^{+\infty} I(\Phi_B, V) P(\Phi_B)\, \mathrm{d}\Phi \tag{10}$$

where $I(\Phi_B, V)$ is the current at a bias V for a barrier of height based on the ideal TED theory and $P(\Phi_B)$ is the normalized distribution function giving the probability of the accuracy for the barrier height.

Now, introducing $I(\Phi_B, V)$ and $P(\Phi_B)$ into equation (10) from (1) and (9), and performing the integration from $-\infty$ to $+\infty$, one can obtain the current $I(V)$ through a Schottky barrier at a forward bias V, similar to equations (1) and (2) but with the modified barrier:

$$I(V) = A^*T^2 \exp\left[-\frac{q}{kT}\left(\bar{\Phi} - \frac{q\sigma_s^2}{2kT}\right)\right] \times \exp\left(\frac{qV}{n_{ap}kT}\right)\left[1 - \exp\left(-\frac{qV}{kT}\right)\right] \tag{11}$$

with

$$I_0 = A\ A^*\ T^2\ \exp\left(-\frac{q\Phi_{ap}}{kT}\right) \tag{12}$$

where Φ_{ap} and n_{ap} are the apparent barrier height and apparent ideality factor, respectively, and are given by [14, 33]

$$\Phi_{ap} = \bar{\Phi}_{B0}(T=0) - \frac{q\sigma_0^2}{2kT} \tag{13}$$

$$\left(\frac{1}{n_{ap}} - 1\right) = \rho_2 - \frac{q\rho_3}{2kT}. \tag{14}$$

It is assumed that the mean SBH $\bar{\Phi}_B$ and σ_s are linearly bias dependent on Gaussian parameters, such as $\bar{\Phi}_B = \bar{\Phi}_{B0} + \rho_2 V$ and standard deviation $\sigma_s = \sigma_{s0} + \rho_3 V$, where ρ_2 and ρ_3 are voltage coefficients which may depend on temperature, quantifying the voltage deformation of the BH distribution [29, 36, 40].

The temperature dependence of σ_s is usually small and can be neglected [40]. It is obvious that the decrease of the zero-bias barrier height is caused by the existence of the Gaussian distribution and the extent of influence is determined by the standard deviation itself. Also, the effect is particularly significant at low temperatures. Fitting of the experimental data in equation (2) or (12) and in equation (3) gives Φ_{ap} and n_{ap} at zero-bias respectively which should obey equations (13) and (14). Thus, the plot of Φ_{ap} versus $q/2kT$ (figure 5) should be a straight line that gives $\bar{\Phi}_B(T=0) = 0.535$ eV and $\sigma_0 = 0.069$ V from the intercept and slope, respectively. The lower value of σ_0 corresponds to more homogeneous BH. Clearly, the diode with the best rectifying performance presents the best barrier homogeneity with the lower value of standard deviation. It was seen that the value of $\sigma_0 = 0.069$ V is not small compared to the mean value of $\bar{\Phi}_B = 0.535$ eV, indicating the presence of interface inhomogeneities. Furthermore, when compared to the temperature dependence of Φ_{ap}, the modified Φ_{bf} is nearly temperature independent. The solid circles in figure 2 represent data estimated with these parameters using equation (13). As was reported in [36–38, 39], barrier inhomogeneities can occur as a result of inhomogeneities in the composition of the interfacial oxide layer thickness. The standard deviation is a measure of the barrier inhomogeneity. The lower value of σ_0 corresponds to a more homogeneous barrier height. Nevertheless, this inhomogeneity and potential fluctuation dramatically affect low temperature I–V characteristics. It is responsible, in particular, for the abnormal behavior in the Richardson plot in figure 4.

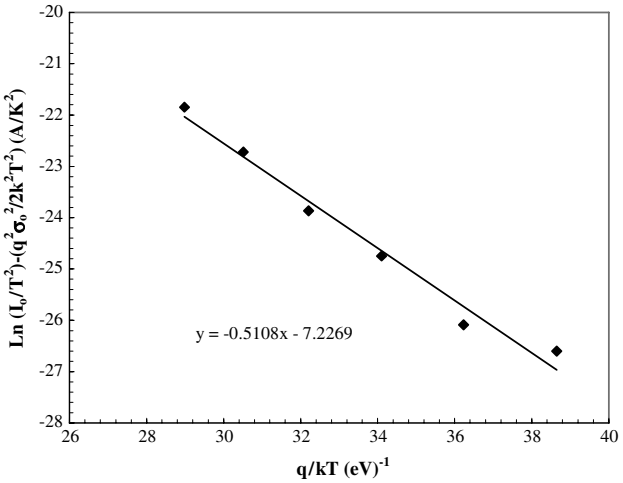

Figure 6. Modified Richardson $\ln(I_0/T^2) - q^2\sigma^2/2kT^2$ versus $1/T$ plot for the Al–TiW–Pd_2Si/n-Si Schottky diode according to the Gaussian distribution of the barrier height.

The temperature dependence of the ideality factor can be understood on the basis of equation (14). Fitting showing the ideality factor n in figure 5 is a straight line that gives voltage coefficients ρ_2 and ρ_3 from the intercept and slope of the plot where $\rho_2 = -0.594$ and $\rho_3 = -0.057$ V from the experimental data. The linear behavior of the plot shows that the ideality factor expresses the voltage deformation of the Gaussian distribution of the SBD.

In figure 4 the plot of $\ln(I_0/T^2)$ versus $1/T$ shows the activation energy and Richardson constant which deviates from the known value. To explain this behavior,

equation (10) can be rewritten by combining equation (12) with (13) as

$$\ln\left(\frac{I_0}{T^2}\right) - \left(\frac{q^2\sigma_0^2}{2k^2T^2}\right) = \ln(AA*) - \frac{q\bar{\Phi}_{B0}}{kT}. \qquad (15)$$

The modified $\ln(I_0/T^2) - q^2\sigma_0^2/2k^2T^2$ versus q/kT plot according to equation (15) should give a straight line with the slope directly yielding the mean $\bar{\Phi}_{B0}$ and the intercept $(=\ln AA*)$ at the ordinate determining $A*$ for a given diode area A (figure 6). In figure 6, the modified $\ln(I_0/T^2) - q^2\sigma_0^2/2k^2T^2$ versus q/kT plot gives $\bar{\Phi}_{B0}$ $(T = 0)$ and $A*$ as 0.510 eV and 121.96 A cm^{-2} K^{-2}, respectively.

4. Conclusion

To investigate whether the top conductor, aluminum, is responsible for the abnormal behavior of the *I–V* characteristic or not, a layer of Ti–W (10% Ti, 90% W) was sputter coated between the palladium silicide and metal interconnects in the fabricating process of the Pd_2Si-based Schottky diode. However, it was shown that the *I–V* characteristics of the Al–TiW–Pd_2Si/n-Si SBD in the temperature range of 300–400 K were found to be a strong function of temperature. The only satisfactory explanation of the *I–V* characteristics of the Al–TiW–Pd_2Si/n-Si SBD in the temperature range of 300–400 K can be made on the basis of TE with Gaussian distribution of the barrier height of $\bar{\Phi}_{B0}(T = 0) = 0.535$ eV and a standard deviation of $\sigma_0 = 0.069$. As is known, the distribution of the barrier height is caused by inhomogeneities that are present at the interface. Furthermore, the experimental results of Φ_{ap} and n_{ap} fit very well for the theoretical equation related to the Gaussian distribution of Φ_{ap} and $n_{ap.}$ Again the $\ln(I_0/T^2)$ versus $1/T$ plots yield an unreasonable effective Richardson constant although the flat-band temperature coefficient was used in the calculation. But the Richardson value of 121.96 A cm^{-2} K^{-2} obtained by means of the modified Richardson plot considering the Gaussian distribution of the barrier heights is very close to the theoretical value of 120 A cm^{-2} K^{-2} for electrons in n-type Si.

References

[1] Kircher C J 1971 *Solid-State Electron.* **14** 507
[2] Wittmer M, Smith D L, Lew P W and Nicolet M A 1978 *Solid-State Electron.* **21** 573
[3] Shepela A 1973 *Solid-State Electron.* **16** 477
[4] Buckley W D and Moss S C 1972 *Solid-State Electron.* **15** 1331
[5] Bower R W, Sigurd D and Scot R E 1973 *Solid-State Electron.* **16** 1461
[6] Lau S S, Chu W K, Mayer J W and Tu K N 1974 *Thin Solid Films* **23** 205
[7] Fertig D J and Robinson G Y 1976 *Solid-State Electron.* **19** 407
[8] Olowolafe J O, Nicolet M A and Mayer J W 1977 *Solid-State Electron.* **20** 413
[9] Köster U, Campbell D R and Tu K N 1978 *Thin Solid Films* **53** 129
[10] Ishiwara H, Hikosaka K, Nagatomo M and Furukawa S 1979 *Surf. Sci.* **86** 711
[11] Ho P S, Rubloff G W, Lewis J E, Moruzzi V L and Williams A R 1980 *Phys. Rev.* B **22** 4784
[12] Studer B 1980 *Solid-State Electron.* **23** 1181
[13] Föll H and Ho P S 1981 *J. Appl. Phys.* **52** 5510
[14] Finstad T G and Nicolet M A 1980 *Thin Solid Film* **68** 393
[15] Eizenberg M, Foell H and Tu K N 1981 *J. Appl. Phys.* **52** 861
[16] Elabd H, Villani T S and Kosonocky W F 1982 *IEEE Trans. Electron Devices Lett.* **3** 89
[17] Kosonocky W F and Elabd H 1983 *SPIE* **443** 167
[18] Kosonocky W F, Shallcros F V, Villani T S and Groppe J V 1985 *IEEE Trans. Electron Devices Lett.* **32** 564
[19] Eriksson M and Ekedahl L-G 1998 *J. Appl. Phys.* **83** 3947
[20] Chand S and Kumar J 1996 *J. Appl. Phys.* **80** 288
[21] Chand S and Kumar J 1996 *Semicond. Sci. Technol.* **11** 1203
[22] Chand S and Kumar J 1997 *Appl. Phys.* A **65** 497
[23] Chand S and Kumar J 1996 *Appl. Phys.* A **63** 171
[24] Afandiyeva İ M, Dökme İ, Altındal Ş, Abdullayeva L K and Askerov Sh G 2008 *Microelectron. Eng.* **85** 367
[25] Sullivan J P, Tung R T, Pinto M R and Graham W R 1991 *J. Appl. Phys.* **70** 7403
[26] Doğan H, Korkut H, Yıldırım N and Türüt A 2007 *Appl. Surf. Sci.* **253** 7467
[27] Tung R T 2001 *Mater. Sci. Eng.* R **35** 1
[28] Card H C and Rhoderick E H 1971 *J. Phys. D: Appl. Phys.* **4** 1589
[29] Zhu S, Detavernier C, Van Meirhaeghe R L, Cardon F, Ru G P, Qu X P and Li B Z 2000 *Solid-State Electron.* **44** 1807
[30] Cova P and Singh A 1990 *Solid-State Electron.* **33** 11
[31] Dökme İ 2007 *Physica B: Cond. Mater.* **388** 10
[32] Altındal Ş, Dökme İ, Bülbül M M, Yalçın N and Serin T 2006 *Microelectron. Eng.* **83** 499
[33] Dökme İ and Altındal Ş 2006 *Semicond. Sci. Technol.* **21** 1053–8
[34] Schmitsdorf R F, Kampen T U and Mönch W 1995 *Surf. Sci.* **324** 249
[35] Werner J H and Guttler H H 1991 *Physica Scripta* T **39** 258
[36] Dökme İ, Altındal Ş and Bülbül M M 2006 *Appl. Surf. Sci.* **252** 7749
[37] Song Y P, Van Meirhaeghe R L, Laflere W H and Cardon F 1986 *Solid-State Electron.* **29** 663
[38] Gümüş A, Türüt A and Yalçın N 2002 *J. Appl. Phys.* **91** 245
[39] Werner J H and Guttler H H 1991 *Appl. Phys.* **69** 1522
[40] Hudait M K, Venkateswarlu S P and Krupanidhi S B 2001 *Solid-State Electron.* **45** 133
[41] Roccaforte F R, La Via F, Baari A and Raineri V 2004 *J. Appl. Phys.* **96** 4313
[42] Roccaforte F R, Lucolana F, Giannazzo F, Alberti A and Raineri V 2006 *Appl. Phys. Lett.* **89** 022103